



Genome of the pitcher plant *Cephalotus* reveals genetic changes associated with carnivory

Fukushima, Kenji; Fang, Xiaodong; Alvarez-Ponce, David; Cai, Huimin; Carretero-Paulet, Lorenzo; Chen, Cui; Chang, Tien-Hao; Farr, Kimberly M.; Fujita, Tomomichi; Hiwatashi, Yuji; Hoshi, Yoshikazu; Imai, Takamasa; Kasahara, Masahiro; Sanz, Pablo Librado; Mao, Likai; Mori, Hitoshi; Nishiyama, Tomoaki; Nozawa, Masafumi; Pálfalvi, Gerg; Pollard, Stephen T.; Rozas, Julio; Sánchez-Gracia, Alejandro; Sankoff, David; Shibata, Tomoko F.; Shigenobu, Shuji; Sumikawa, Naomi; Uzawa, Taketoshi; Xie, Meiyang; Zheng, Chunfang; Pollock, David D.; Albert, Victor A.; Li, Shuaicheng; Hasebe, Mitsuyasu

Published in:

Nature Ecology and Evolution

DOI:

[10.1038/s41559-016-0059](https://doi.org/10.1038/s41559-016-0059)

Publication date:

2017

Document version

Publisher's PDF, also known as Version of record

Document license:

[CC BY](#)

Citation for published version (APA):

Fukushima, K., Fang, X., Alvarez-Ponce, D., Cai, H., Carretero-Paulet, L., Chen, C., Chang, T.-H., Farr, K. M., Fujita, T., Hiwatashi, Y., Hoshi, Y., Imai, T., Kasahara, M., Sanz, P. L., Mao, L., Mori, H., Nishiyama, T., Nozawa, M., Pálfalvi, G., ... Hasebe, M. (2017). Genome of the pitcher plant *Cephalotus* reveals genetic changes associated with carnivory. *Nature Ecology and Evolution*, 1(3), [0059]. <https://doi.org/10.1038/s41559-016-0059>

Genome of the pitcher plant *Cephalotus* reveals genetic changes associated with carnivory

Kenji Fukushima^{1,2,3*}, Xiaodong Fang^{4,5†}, David Alvarez-Ponce⁶, Huimin Cai^{4,5}, Lorenzo Carretero-Paulet^{7,8}, Cui Chen⁴, Tien-Hao Chang⁸, Kimberly M. Farr⁸, Tomomichi Fujita⁹, Yuji Hiwatashi¹⁰, Yoshikazu Hoshi¹¹, Takamasa Imai¹², Masahiro Kasahara¹², Pablo Librado^{13,14}, Likai Mao⁴, Hitoshi Mori¹⁵, Tomoaki Nishiyama¹⁶, Masafumi Nozawa^{1,17}, Gergő Pálfalvi^{1,2}, Stephen T. Pollard³, Julio Rozas¹³, Alejandro Sánchez-Gracia¹³, David Sankoff¹⁸, Tomoko F. Shibata^{1,19}, Shuji Shigenobu^{1,2}, Naomi Sumikawa¹, Taketoshi Uzawa²⁰, Meiyang Xie⁴, Chunfang Zheng¹⁸, David D. Pollock³, Victor A. Albert^{8*}, Shuaicheng Li^{4,5*} and Mitsuyasu Hasebe^{1,2*}

Carnivorous plants exploit animals as a nutritional source and have inspired long-standing questions about the origin and evolution of carnivory-related traits. To investigate the molecular bases of carnivory, we sequenced the genome of the heterophyllous pitcher plant *Cephalotus follicularis*, in which we succeeded in regulating the developmental switch between carnivorous and non-carnivorous leaves. Transcriptome comparison of the two leaf types and gene repertoire analysis identified genetic changes associated with prey attraction, capture, digestion and nutrient absorption. Analysis of digestive fluid proteins from *C. follicularis* and three other carnivorous plants with independent carnivorous origins revealed repeated co-options of stress-responsive protein lineages coupled with convergent amino acid substitutions to acquire digestive physiology. These results imply constraints on the available routes to evolve plant carnivory.

Carnivorous plants bear extensively modified leaves capable of attracting, trapping and digesting small animals, and absorbing the released nutrients^{1,2}. Plant carnivory evolved independently in several lineages of flowering plants, providing a classic model for the study of convergent evolution³. *Cephalotus follicularis* (*Cephalotus*), a carnivorous plant native to southwest Australia that belongs to the monospecific family Cephalotaceae in the order Oxalidales, forms both carnivorous pitcher leaves and non-carnivorous flat leaves (Fig. 1). Co-existence of the two types of leaf in a single individual plant provides a unique opportunity to understand the genetic basis of plant carnivory through comparative analysis of these serially homologous organs. To this end, we sequenced the *Cephalotus* genome. A total of 305 Gb of Illumina reads were generated for contig assembly and scaffolding, and 17 Gb of PacBio reads for inter-contig gap filling (Supplementary Table 1). The resulting assembly consists of 16,307 scaffolds totaling 1.61 Gb with an N50 length of 287 kb (Supplementary Table 2),

corresponding to 76% of the estimated genome size (Supplementary Fig. 1a). Long-terminal repeat retrotransposons account for 76% of the genome (Supplementary Tables 3 and 4). Syntenic block comparison with the robusta coffee genome, which maintained diploidy since the ancient split from the *Cephalotus* lineage⁴, reveals mostly one-to-one mappings (Fig. 1c and Supplementary Table 5), indicating that the *Cephalotus* genome has not experienced further whole genome duplications since the hexaploidy event at the origin of core eudicots⁵ (Supplementary Note 1). We annotated 36,503 protein-coding genes (Supplementary Fig. 1b–e), and 72 microRNA (miRNA) loci (Supplementary Table 6) and their potential targets (Supplementary Table 7) using RNA-sequencing (RNA-seq) data of representative tissues (Supplementary Tables 8–10). Orthologous gene groups (orthogroups) were defined using OrthoMCL⁶ for the complete gene sets of *Cephalotus* and eight eudicot species (Supplementary Tables 11 and 12). Analysis of shared singletons indicates that core eudicot genes are

¹National Institute for Basic Biology, Okazaki 444-8585, Japan. ²Department of Basic Biology, School of Life Science, SOKENDAI (Graduate University for Advanced Studies), Okazaki 444-8585, Japan. ³Department of Biochemistry and Molecular Genetics, University of Colorado School of Medicine, Aurora, Colorado 80045, USA. ⁴BGI-Shenzhen, Shenzhen 518083, China. ⁵Department of Computer Science, City University of Hong Kong, Hong Kong 999077, China. ⁶Department of Biology, University of Nevada, Reno, Nevada 89557, USA. ⁷Department of Plant Systems Biology, VIB, Ghent University, Ghent 9002, Belgium. ⁸Department of Biological Sciences, University at Buffalo, Buffalo, New York 14260, USA. ⁹Department of Biological Sciences, Faculty of Science, Hokkaido University, Sapporo 060-0810, Japan. ¹⁰School of Food, Agricultural and Environmental Sciences, Miyagi University, Miyagi 982-0215, Japan. ¹¹Department of Plant Science, School of Agriculture, Tokai University, Kumamoto 869-1404, Japan. ¹²Department of Computational Biology and Medical Sciences, Graduate School of Frontier Sciences, The University of Tokyo, Kashiwa 277-8568, Japan. ¹³Departament de Genètica and Institut de Recerca de la Biodiversitat (IRBio), Universitat de Barcelona, Diagonal 643, Barcelona 08028, Spain. ¹⁴Center for GeoGenetics, Natural History Museum of Denmark, University of Copenhagen, 1350K Copenhagen, Denmark. ¹⁵Graduate School of Bioagricultural Sciences, Nagoya University, Nagoya 464-8601, Japan. ¹⁶Advanced Science Research Center, Kanazawa University, Kanazawa 920-0934, Japan. ¹⁷Department of Biological Sciences, Tokyo Metropolitan University, Hachioji 192-0397, Japan. ¹⁸Department of Mathematics and Statistics, University of Ottawa, K1N 6N5 Ottawa, Canada. ¹⁹Tohoku Medical Megabank Organization, Tohoku University, Sendai 980-8573, Japan. ²⁰Department of Natural Science, Osaka Kyoiku University, Osaka 582-8582, Japan. *These authors contributed equally to this work. *e-mail: kenji.fukushima@ucdenver.edu; vaalbert@buffalo.edu; shuaicli@cityu.edu.hk; mhasebe@nibb.ac.jp

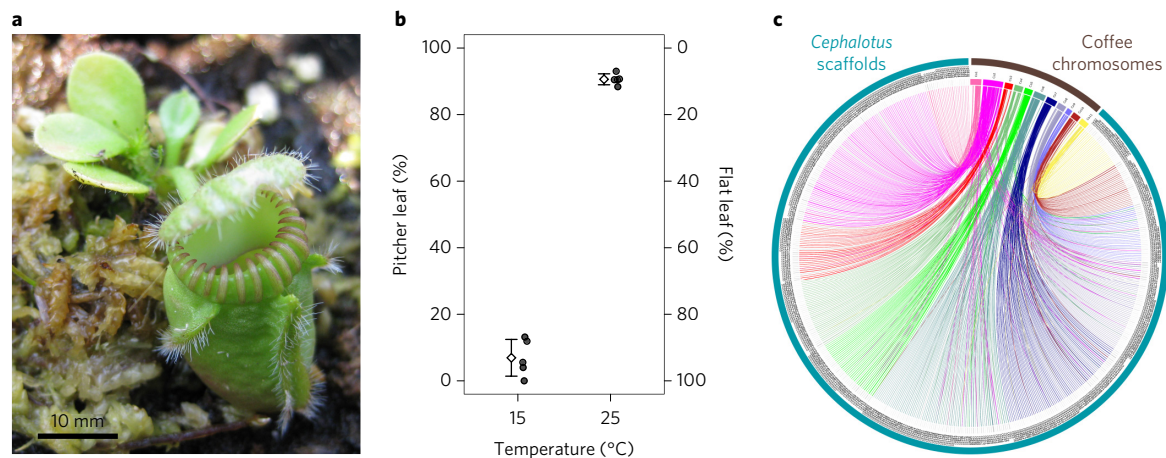


Figure 1 | *Cephalotus* morphology and genome. **a, Pitcher and flat leaves. **b**, Flat and pitcher leaves predominantly produced at 15 °C and 25 °C, respectively, under continuous light conditions. Diamonds and error bars indicate means and standard deviations, respectively. Each filled circle represents an independent experiment with 45 plants. **c**, Synteny block matching of the *Cephalotus* genome against the coffee genome⁴ revealed a one-to-one matching in most genomic loci.**

conserved in the *Cephalotus* genome (Supplementary Note 2 and Supplementary Table 13).

Maximum-likelihood gene gain and loss analysis detected lineage-specific expansion of 492 orthogroups in *Cephalotus* (Supplementary Table 14). Gene ontology (GO) enrichment analysis (Supplementary Tables 15–21) highlighted *Cephalotus*-expanded orthogroups containing purple acid phosphatases, known as a typical component of digestive fluids^{1,7} (Supplementary Table 17). RNase T2, also known as a constituent of digestive fluids^{1,8,9}, is enriched among orthogroups composed only of genes from *Cephalotus* and another carnivorous plant *Utricularia gibba* (Supplementary Table 18). Also, the enriched GO term ‘cellular response to nitrogen levels’ included ten *Cephalotus*-specific singleton genes encoding dihydropyrimidinases, which have the potential function of acquired nitrogen recycling (Supplementary Table 19). Nitrogen is, in turn, known to be one of the primary limiting nutrients that carnivorous plants derive from prey^{1,10}.

As we succeeded in regulating the developmental switch between pitcher and flat leaves by ambient temperature (Fig. 1b and Supplementary Fig. 1f,g), their transcriptomes were compared. The pitcher transcriptome was differentially enriched with cell cycle- and morphogenesis-related GO terms (Supplementary Table 22), which may reflect the morphological complexity of pitcher leaves. Although both developmental and thermoresponsive genes may change their expression in the temperature-dependent leaf switching, certain developmental regulators related to adaxial–abaxial polarity (for example, *AS2*, *YAB5*, and *WOX1* orthologues) showed higher expression levels in shoot apices bearing pitchers than those terminating in flat leaves (Supplementary Fig. 2), implying the involvement of such factors in pitcher development and evolution. In contrast, the flat leaf transcriptome was enriched with photosynthesis-related GO terms (Supplementary Table 23). These results are compatible with the distinct functional specializations of carnivory-dominated pitcher leaves versus photosynthesis-dominated flat leaves.

Carnivorous plants attract potential prey by nectar, coloration and scent^{1,11,12}. GO terms enriched in the pitcher transcriptome included ‘starch metabolic process’ and ‘sucrose metabolic process’ (Supplementary Table 22), which may be related to the production of attractive nectar. Indeed, we detected transcriptional upregulation of certain sucrose biosynthetic genes and members of sugar efflux carriers in pitcher leaves (Supplementary Fig. 3).

The epidermis of carnivorous pitfall traps often develops a slippery, waxy surface that promotes prey capture and prevents them from

escaping^{1,13}. A cytochrome P450 (CYP) orthogroup was expanded in the *Cephalotus* lineage (Supplementary Table 14). In a phylogenetic tree, these CYP genes belonged to a clade containing *Arabidopsis* genes involved in wax and cutin biosynthesis (*CYP86* and *CYP96A*)¹⁴ (Supplementary Fig. 4). These genes, as well as wax ester synthase orthologues (*WSD1*)¹⁵, showed pitcher-pre-dominant expression and are tandemly duplicated in the genome (Supplementary Fig. 4), suggesting possible co-regulated involvement of the clusters in slippery surface formation.

Carnivorous plants secrete digestive enzymes for degradation of trapped animals^{1,11,12}. Previous studies on several digestive enzymes of *Nepenthes* spp., *Drosera* spp., *Dionaea muscipula* and *Cephalotus* indicate that pathogenesis-related proteins were co-opted for digestive function as well as for preventing microbial colonization of digestive fluid (refs^{16–19} and refs in Supplementary Table 24). To further investigate the origin and evolution of digestive enzymes of *Cephalotus* and three other distantly related carnivorous plants (*Drosera adelae*, *N. alata* and *Sarracenia purpurea*), we sequenced fragments of digestive fluid proteins and identified 35 corresponding genes (Fig. 2a and Supplementary Tables 25–28). As *Drosera* and *Nepenthes* trace back to a common carnivorous origin in Caryophyllales^{3,20}, the four species including *Cephalotus* therefore cover three independent origins of plant carnivory. Together with previously identified enzyme sequences including proteins from *Dionaea* (Supplementary Table 24), we inferred phylogenetic relationships among the digestive fluid proteins (Fig. 2b and Supplementary Fig. 5a–ah). Glycoside hydrolase family 19 (GH19) chitinase, β -1,3-glucanase, PR-1-like protein, thaumatin-like protein, purple acid phosphatase and RNase T2 genes showed orthologous relationships among carnivores despite their multiple origins. This result suggests that orthologous genes were repeatedly co-opted for digestive functions in independent carnivorous plant lineages.

To infer putative ancestral functions of these independently arisen digestive fluid proteins, we examined the expression patterns of their phylogenetically most closely related *Arabidopsis* genes (Supplementary Fig. 5a–ah). Compared with other genes in the same families, these *Arabidopsis* genes showed a significant tendency to be upregulated on various biotic and abiotic stresses ($P < 0.02$, randomization test) (Supplementary Fig. 5ai). This result suggests that co-option from stress-responsive proteins is a general evolutionary trend in the repeated evolution of carnivorous plant enzymes. Whether they are currently bifunctional—having both carnivorous and non-carnivorous roles—is unclear, but tissue-specific

basal expression is probably optimized for carnivory in *Cephalotus* and *N. alata*, as the genes are preferentially expressed in their pitcher traps (Fig. 2c,d).

In *Cephalotus*, three aspartic proteases were identified in the digestive fluid proteome. We found three genomic clusters of aspartic

protease genes containing both pitcher-preferential and constitutively expressed genes (Supplementary Fig. 5a–c). Together with the inferred tandem duplications of *CYP*, this result highlights the roles of gene duplication and subsequent functional divergence in carnivorous plant evolution.

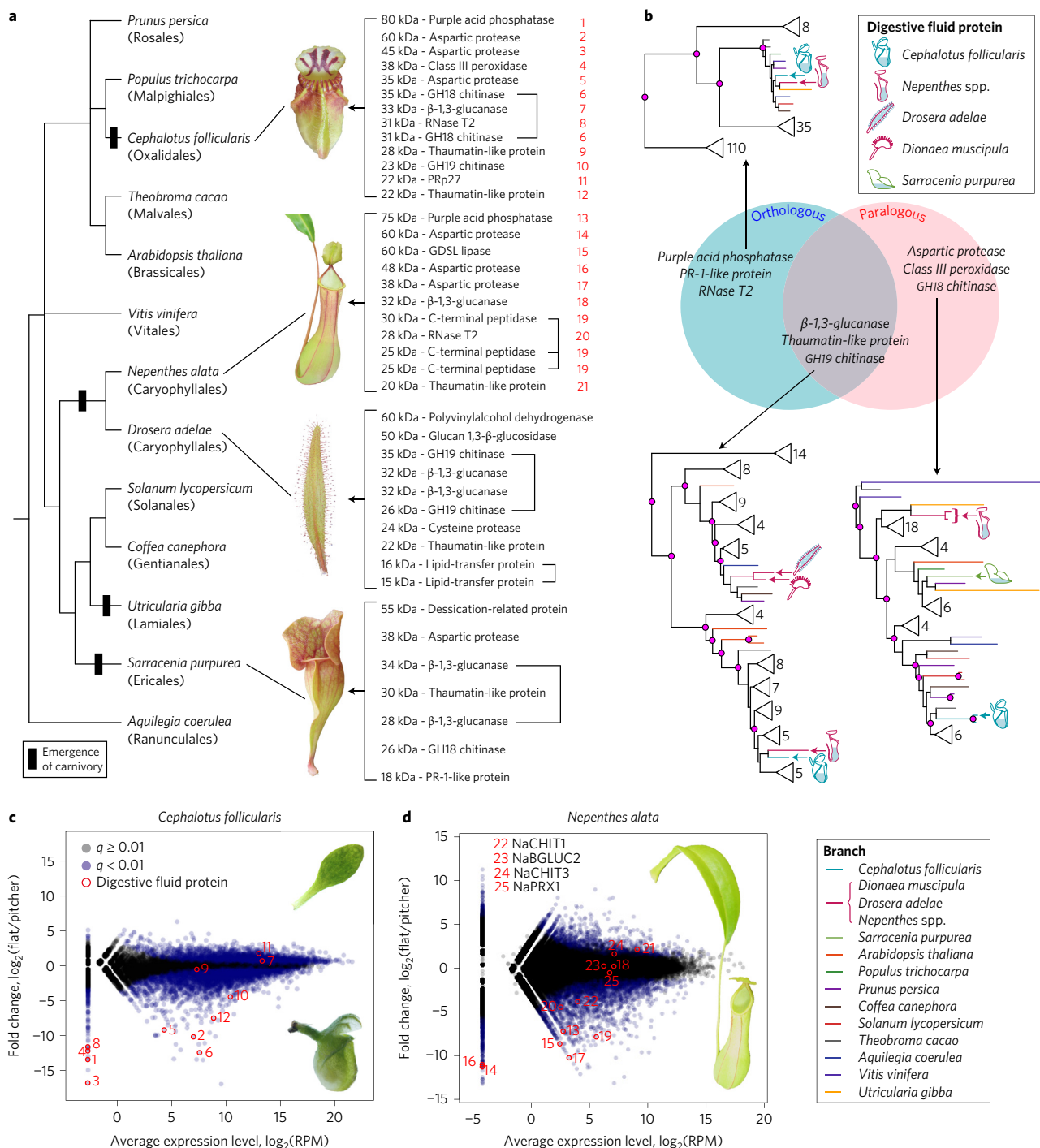


Figure 2 | Orthologue-paralogue relationships and carnivory-related expression of digestive fluid proteins. **a**, Phylogenetic relationships of independently evolved carnivorous plants and, to their right, the digestive fluid proteins identified through proteomic analysis. Polytoomy in the tree represents topological discrepancy between previously reported plastid and nuclear phylogenies (see Methods). Brackets connect protein variants likely to originate from the same gene. **b**, Phylogeny-based orthologue-paralogue classification. Branch colours denote species identities. Magenta on internal nodes indicates inferred duplication events. Gene numbers in collapsed clades are shown next to triangles. The collapsed clades do not contain genes encoding the digestive fluid proteins but may contain other *Cephalotus* genes as well as non-carnivorous plant genes. Complete trees are available in Supplementary Fig. 5. **c,d**, Transcriptome comparison of flat and pitcher organs in *Cephalotus* (**c**) and *N. alata* (**d**). Red numbers indicate positions of genes encoding digestive fluid proteins identified in this work (1–21, shown in **a**) and previous studies (22–25, Supplementary Table 24), several of which are outliers showing trap-specific expression.

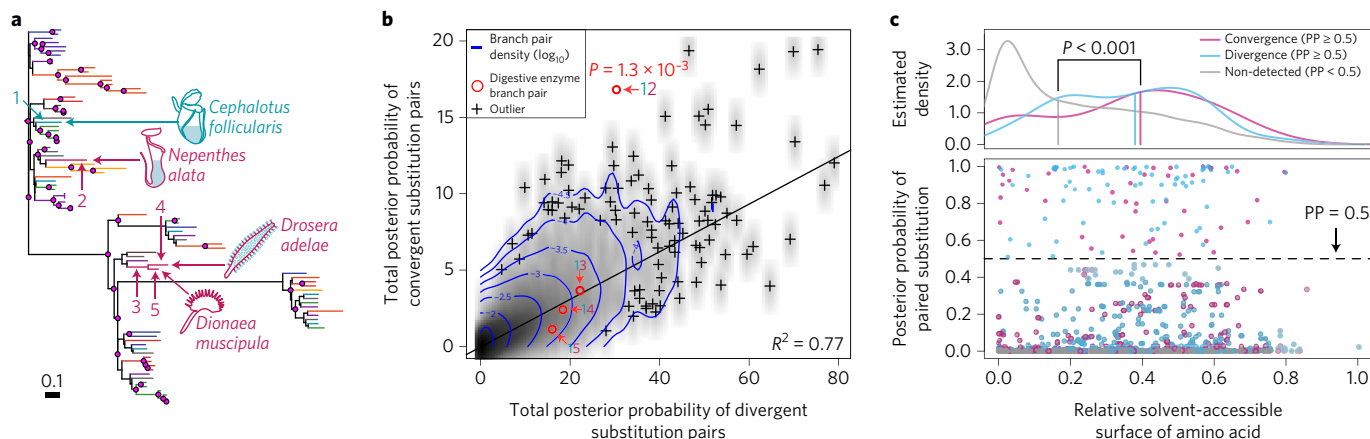


Figure 3 | Molecular convergence of digestive enzymes. **a**, GH19 chitinase phylogeny obtained from the phylogeny reconciliation. Identified digestive enzyme genes are indicated by trap illustrations. Magenta on internal nodes indicates inferred duplication events. The bar indicates 0.1 nucleotide substitutions per site. The complete tree is available in Supplementary Fig. 6q. **b**, Accumulation of convergent amino acid substitutions in GH19 chitinases. The positions of digestive enzyme branch pairs are indicated by red circles with corresponding numbers in **a**. Grey tones indicate branch pair density. The line shows a linear regression. **c**, Relationships between substitution processes and amino acid exposure in protein structures. As the convergent branch pairs in different families showed similar patterns (Supplementary Fig. 8e), data from GH19 chitinases, purple acid phosphatases and RNase T2s are pooled. The bottom panel shows posterior probabilities (PP) of convergent (pink) and divergent (light blue) substitution pairs. The top panel shows density distributions of convergent and divergent loci (PP ≥ 0.5 , filled pink and light blue in the lower panel) as well as non-detected positions (PP < 0.5 , filled grey with outline colour according to the substitution types). P value indicates a statistical difference of medians (vertical lines) (randomization test).

The repeated evolutionary utilization of similar genes may have been accompanied by convergent responses to carnivory-specific selective pressures at the amino acid substitution level. To test this, we developed a tree-based method for the detection of molecular convergence in multigene families, using phylogeny reconciliation between third codon position-derived gene trees and a consensus species tree (Supplementary Note 3, see Methods for the choice of a species tree). Using reconciled trees, the number of digestive enzyme-specific convergent substitutions was inferred on the basis of Bayesian ancestral sequence reconstructions (Fig. 3a,b and Supplementary Fig. 6). By comparing convergent substitution numbers and empirically calculated background-level expectations²¹, we found that GH19 chitinases (Fig. 3a,b), purple acid phosphatases (Supplementary Fig. 6i,j) and RNase T2s (Supplementary Fig. 6m,n) significantly accumulated convergent amino acid substitutions. For all three enzymes, two pitfall-type carnivorous pitcher plants, *Cephalotus* and *N. alata*, were associated as convergent branch pairs. Furthermore, for RNase T2, significant molecular convergence was also detected between *Cephalotus* and the common ancestor of the three Caryophyllales species, *D. adelae*, *D. muscipula* and *N. alata*, which produce sticky, snap and pitfall traps, respectively. Parsimonious inference of character evolution indicates that trapping strategy diversified after the establishment of carnivory in the Caryophyllales^{3,20}. Therefore, molecular adaptation of RNase T2 probably occurred both during the evolution of carnivory and subsequently during the establishment of the specific capture strategy of pitfall traps. It is noteworthy that the *Cephalotus* RNase T2 and purple acid phosphatase genes are located adjacent to each other within a 40 kb interval of the *Cephalotus* genome (Supplementary Fig. 7). This placement could indicate an arrangement favoured by adaptive, positionally correlated co-expression²² of these modified carnivorous enzymes (Supplementary Note 4). In light of similar cases of convergent evolution shown for animal digestive enzymes^{23,24}, we propose that major changes in nutritional strategy impose a selective pressure strong enough to override evolutionary contingency in both plants and animals.

As protein structure imposes major constraints on amino acid substitutions^{25–27}, we mapped amino acid residues identified as convergent onto corresponding 3D enzyme models. Convergent

positions do not overlap with or cluster around catalytically essential amino acids (Supplementary Fig. 8). Instead, they tend to be located at exposed positions to an extent comparable to divergent substitutions (Fig. 3c), despite the prediction that more exposed positions result in lower convergence probability²⁸. Exposed sites are structurally less constrained, and substitutions in such sites are likely to change their interactions with other molecules in solution, rather than changing protein conformation^{25–27}. During the evolution of digestive enzymes, selective pressures may have come from the digestive fluid environment, which include the presence of insect-derived substrates, high endogenous proteolytic activity, low pH and microbial invasion or symbiosis^{1,11,12}. As exposed residues constitute the protein–environment interface, the convergent amino acid substitutions may have been critical factors for the convergent establishment of carnivory across the angiosperms.

In the final phase of carnivorous plant physiology, digested molecules are absorbed into the plant body to promote growth and reproduction^{1,29}. We found that various transporters were preferentially expressed in pitcher leaves (Supplementary Table 29). One pitcher-predominant transporter showed phylogenetic affinity to the AMMONIUM TRANSPORTER 1 (AMT1) subfamily (Supplementary Fig. 9), which contains the previously characterized carnivory-related *D. muscipula* gene *DmAMT1*³⁰. This result, together with the repeated co-option of digestive enzymes already described, indicates utilization of common genetic programs and evolutionary pathways in independently evolved carnivorous plant lineages.

The *Cephalotus* genome has allowed us to discover numerous genes associated with evolutionary transition to carnivory in plants. In particular, the high degree of convergent evolution in digestive enzymes indicates that there are few available evolutionary pathways for angiosperms to become carnivorous.

Methods

Plant materials and culture conditions. Axenically grown plants of *C. follicularis* were obtained from CZ Plants Nursery (Trebovice, Czech Republic) and were maintained in polycarbonate containers (60 × 60 × 100 mm) containing half-strength Murashige and Skoog solid medium³¹ supplemented with 3% sucrose, 1× Gamborg's vitamins, 0.1% 2-(N-morpholino)ethanesulfonic acid, 0.05% Plant Preservative Mixture (Plant Cell Technology) and 0.3% Phytigel,

at 25°C in continuous light. For transcriptome sequencings, *D. adalae* was cultivated in a peat pot in an incubator at 25°C in continuous light. *N. alata* was grown in soil in a greenhouse. *S. purpurea* was grown in peat-based soil and was maintained in a field. For digestive fluid sampling, *C. follicularis*, *D. adalae*, *N. alata* and *S. purpurea* were grown in a greenhouse.

Culture conditions for leaf fate regulation. Shoot apices with one or two expanded leaves were collected with fine forceps from plants grown at 25°C and planted on medium. The plantlets were grown for 12 weeks under a light intensity of 20–40 $\mu\text{mol m}^{-2} \text{s}^{-1}$. Numbers of youngest pitcher and flat leaves on main shoots were counted for each plantlet (Fig. 1b). Leaves with intermediate shapes were counted as either of the two categories based on morphological similarity.

DNA isolation. Total genomic DNA was isolated from young flat leaves and pitcher leaves of axenically grown plants. Collected leaves were homogenized in liquid nitrogen using a mortar and pestle. The homogenate was transferred into 2× CTAB extraction buffer (2% cetyltrimethylammonium bromide (CTAB), 1.4 M NaCl, 100 mM Tris-HCl (pH 8.0), 20 mM EDTA (pH 8.0)) preheated to 80°C and was gently agitated at 60°C for 1 h. An equal volume of chloroform:isoamyl alcohol (25:1) was added and agitated using a rotator at 20 r.p.m. for 10 min at room temperature. After centrifugation at 9,000 × g for 30 min at room temperature, supernatants were transferred to new tubes and supplemented with 1/10 volume of 10% CTAB and an equal volume of chloroform:isoamyl alcohol (25:1). The tubes were shaken with a rotator for 10 min. After centrifugation, supernatants were again transferred to new tubes and an equal volume of isopropanol was added. The tubes were centrifuged and supernatants were discarded. The crude DNA pellet was rinsed with 5 ml of 70% EtOH and air-dried for 10 min. The pellet was dissolved in 200 μl of TE (pH 8.0) containing 0.1 mg/ml RNase A, and gently agitated for 60 min at 37°C. A 1/20 volume of 20 mg ml⁻¹ Proteinase K was added, and tubes were incubated at 56°C for 30 min. Subsequently, the DNA solution was further purified using Qiagen Genomic-tip, following the manufacturer's instructions. DNA concentration was determined using fluorometry with Qubit 2.0 (Life Technologies).

Genome sequencing. Whole-genome shotgun short-read sequences were generated with an Illumina HiSeq 2000 to a depth of approximately 150-fold of the 2 Gb *Cephalotus* genome using paired-end and mate-pair protocols, according to the manufacturer's instructions (Supplementary Table 1). For long read sequencing, genomic DNA samples were sheared to 6 kb or 10 kb using g-Tube (Covaris, Massachusetts). Libraries were prepared with DNA Template Prep Kit 2.0 (Pacific Biosciences, California) (3–10 kb) following the manufacturer's instructions and sequencing was performed using PacBio RS with C2 chemistry, P2 polymerase and 45-min movies. Using 158 cells, a total of ca. 17 Gb were generated with a quality cut-off value of 0.75 (Supplementary Table 1).

Genome size estimation. The size of the *Cephalotus* genome was estimated by k-mer frequency analysis using JELLYFISH³² (Supplementary Fig. 1a).

Genome assembly. Illumina paired-end reads with all insert sizes, and mate-pair reads with insert sizes of 2 and 5 kb, were first assembled into 43,308 scaffolds using Allpaths-LG v42381³³. Fragment filling was applied to paired-end libraries with insert sizes of 170 bp and 250 bp. Standard deviations of insert sizes were set to 10% of insert sizes. Gap filling and further scaffolding were performed by adding mate-pair reads with longer inserts using SSPAC³⁴ and GapCloser³⁵. PacBio reads were subjected to two rounds of error correction using Sprai v0.2.2.3 (<http://zombie.cb.ku-tokyo.ac.jp/sprai/>) and used for four rounds of iterative gap filling with PBjelly v12.9.14³⁶. The final assembly included 16,307 scaffolds with N50 of 287 kb (Supplementary Table 2).

Repeat identification. Repetitive elements of the *Cephalotus* genome were first identified and masked for gene prediction (Supplementary Tables 3 and 4). *De novo* prediction of transposable elements was performed using RepeatModeler (<http://www.repeatmasker.org/RepeatModeler.html>) and LTR_FINDER (http://tlife.fudan.edu.cn/ltr_finder/). Known transposable elements were found using RepeatMasker and RepeatProteinMask (<http://repeatmasker.org>). Tandem repeat sequences were screened using Tandem Repeats Finder³⁷.

RNA extraction. Plant materials were ground in liquid nitrogen using a mortar and pestle. Total RNA was extracted using the PureLink Plant RNA Reagent (Life Technologies) and subsequently purified using the RNeasy Mini Kit (QIAGEN). DNase treatment was performed during the column purification. Total RNA was qualified using a 2100 Bioanalyzer (Agilent).

Transcriptome sequencing. Extracted RNA was subjected to two rounds of mRNA enrichment using Dynabeads mRNA Purification Kit (Life Technologies) according to the manufacturer's instructions. RNA-seq libraries were prepared using TruSeq RNA Sample Preparation kit v.2 (Illumina). Strand-specific mRNA libraries were constructed using the dUTP second-strand marking method³⁸. These libraries were sequenced on an Illumina HiSeq 2000 with three biological replications (Supplementary Table 8).

Gene prediction. For gene predictions, we used homology-based, *ab initio* and transcript-based methods. Protein data sets of *Arabidopsis thaliana*, *Linum usitatissimum*, *Manihot esculenta*, *Populus trichocarpa* and *Ricinus communis* (Supplementary Table 11) were aligned to the *Cephalotus* genome using tblastn (cut-off: 1e-5) and then homology-based gene predictions were generated using GeneWise³⁹. We also used Augustus (<http://augustus.gobics.de/>), GENSCAN (<http://genes.mit.edu/GENSCAN.html>), GlimmerHMM (<https://ccb.jhu.edu/software/glimmerhmm/>) and SNAP (<http://korlab.ucdavis.edu/software.html>) for *ab initio* predictions, with model parameters trained using 730 *Cephalotus* gene models that were well supported by homology evidence. RNA-seq data generated from 16 samples (Supplementary Table 8) were used for transcript-based predictions with the Bowtie-Tophat-Cufflinks pipeline⁴⁰. These models were merged using GLEAN (<http://glean-gene.sourceforge.net/>). Finally, gene models that were not in the GLEAN non-redundant gene set but supported by both homology and RNA-seq evidences, or homology-based models (frame shift mutation not allowed and aligning rate >50%), or RNA-seq models encoding proteins ≥ 120 amino acids in length, were further added.

Gene annotation. Gene functions were assigned using BLAST searches (E-value cut-off of 10⁻⁵) against the following databases: KEGG (Release 58), nr (NCBI release 20130904), Swissprot and TrEMBL (Uniprot release 201203). Conserved protein domains were assessed by InterPro⁴¹ and InterProScan⁴² with applications including HMMProfam, HMMPanther, ProfileScan, HMMSmart, FPrintScan and BlastProDom.

Evaluation of genome assembly and gene prediction. Gene coverage of predicted gene sets was evaluated using CEGMA 2.4⁴³ (Supplementary Fig. 1b). Read mapping rates of 15 RNA-seq libraries from five tissues ranged from 74.4% to 83.6% (Supplementary Table 9), indicating consistency between the assembled genome and the sequenced transcriptome.

Small RNA extraction and sequencing. Plant tissues were ground in liquid nitrogen using a mortar and pestle. Total RNA was extracted using PureLink Plant RNA Reagent (Life Technologies) and subsequently purified using the miRNeasy kit (QIAGEN). DNase treatment was performed during the column purification. Briefly, for each sample, RNA of the desired size range (18–30 nucleotides) was size-fractionated and ligated with the 5' adapter and, subsequently, the 3' adapter. Ligated RNA was then subjected to PCR with reverse transcription (RT-PCR) to produce sequencing libraries. Small RNA-seq was performed on an Illumina HiSeq 2000 (Supplementary Table 10).

miRNA prediction and target prediction. *Cephalotus* miRNA loci were predicted in the genome by both transcriptome- and homology-based methods (Supplementary Table 6). Small RNA-seq reads were mapped onto genomic inverted repeats predicted by EMBOS inverted⁴⁴. miRNA loci were identified from the mapping results using ShortStack v1.2.3⁴⁵. For homology-based prediction, 7,385 mature miRNA sequences of Viridiplantae species were retrieved from miRBase release 20⁴⁶. These miRNA sequences were mapped onto the *Cephalotus* genome using patscan⁴⁷, allowing one mismatch. Putative loci mapped by less than five independent miRNAs were excluded. Secondary structures were identified from flanking regions of mapped loci (± 350 bp) using RNAfold of Vienna RNA Package 2.0⁴⁸, and putative miRNA loci were predicted using miRcheck with default parameters⁴⁹. When putative miRNAs were predicted on both strands of the same loci, the minor locus was collapsed. Putative targets of annotated miRNAs were identified using psRNATarget⁵⁰ using default settings (Supplementary Table 7).

OrthoMCL gene classification. Orthologues were clustered by comparison of protein data sets among *A. thaliana*, *C. follicularis*, *Theobroma cacao*, *Vitis vinifera*, *Prunus persica*, *Coffea canephora*, *Solanum lycopersicum*, *U. gibba* and *P. trichocarpa* using BLASTP (cut-off: 10⁻⁵) and OrthoMCL⁶ (Supplementary Tables 11 and 12). Protein data sets of the nine genomes were BLAST searched against nr (NCBI release 20140407; BLASTP, E-value cut-off of 10⁻⁵). Functional terms (GO and enzyme codes) were then assigned to each query sequence using Blast2GO (<https://www.blast2go.com/>).

Maximum-likelihood inference of orthogroup gains and losses. We estimated the divergence times of the surveyed species using RAxML version 8⁵¹, employing tree topologies published previously^{52–54}. The reported placement of *P. persica* (Rosales) is discrepant between plastid-⁵⁴ and nuclear-based analyses^{52,53}. To account for that, we analysed phylogenetic relationships using the single-copy orthologue alignment (see below). Although the bootstrap supports were low, the maximum-likelihood tree supported the nuclear-based topology (Supplementary Fig. 1h), and therefore we placed *P. persica* as sister to the clade containing *A. thaliana*, *T. cacao*, *P. trichocarpa* and *C. follicularis*. The placement of *V. vinifera* is also different among previously published phylogenies^{52–54}. To account for that, two alternative tree topologies with different placements of *V. vinifera* were assumed in this analysis. For that, we leveraged the amino acid sequence data of all single-copy orthologues, as defined by OrthoMCL (1,836 1:1 orthologues), after excluding all putative TE sequences identified in BLAST searches against

different TE databases (TIGR Plant Repeat Databases⁵⁵, TransposonPSI (<http://transposonpsi.sourceforge.net>) and NCBI's non-redundant (nr) protein database). We then aligned the sequences of each orthogroup with the program M-Coffee⁵⁶ and used trimAl⁵⁷ to automatically remove poorly aligned regions. The best-fit amino acid substitution model for each multiple sequence alignment was selected using ProtTest⁵⁸ and specified in the RAxML analysis under a partitioned scheme. We finally used r8s⁵⁹ to obtain the ultrametric trees required for the BadiRate⁶⁰ analysis, by applying the nonparametric rate smoothing algorithm⁵⁹ to the maximum-likelihood trees and fixing the age of the root to 113 Myr in both cases. This date, a compromise for the two trees we tested, was derived from the average of the 2 BEAST point estimates for the earliest split within the rosid clade (with Vitaceae as one sister lineage), as calculated in ref.⁵⁴ (their Fig. 1 and Table 2). The two trees tested are detailed below.

Tree 1:

((V_vinifera:92.251246,(((T_cacao:72.791098,A_thaliana:72.791098):5.199433,(P_trichocarpa:72.150935,C_follicularis:72.150935):5.839595):5.054431,P_persica:83.044961):9.206285):20.748754,(U_gibba:101.840606,(C_canephora:89.804910,S_lycopersicum:89.804910):12.035696):11.159394).

Tree 2:

((U_gibba:82.830331,(C_canephora:74.586612,S_lycopersicum:74.586612):8.243718):14.783045,(((T_cacao:74.611384,A_thaliana:74.611384):5.510359,(P_trichocarpa:73.737693,C_follicularis:73.737693):6.384050):5.848981,P_persica:85.970724):11.642652):15.386624,V_vinifera:113.000000).

To identify gene families specifically expanded in the *Cephalotus* genome, we followed the method implemented in refs⁴ and ⁶¹, accepting a weighted Akaike information criterion (wAIC) ratio of 2.7 for the best-fit branch model to the second-best-fit model. We ran BadiRate⁶⁰ twice, once for each of the two alternative topologies shown above. Only those families strongly supported as expanded (wAIC ratio > 2.7) under both of the two alternative topologies were considered for further analyses (Supplementary Table 14).

GO enrichment analysis. Supplementary Table 12 shows the per species summary of orthogroups and singletons in nine plant species. Before BadiRate analyses, orthogroups containing sequences with significant similarity to transposable elements (resulting in E-values < 10⁻¹⁵ in TBLASTX searches against sequences of the RepBase v19.12 database⁶²) were filtered out from all nine genomes. The functional categories (generic GO terms) differentially represented among 493, 495 and 492 *Cephalotus*-specific expanded genes families (grouping 2,560, 2,567 and 2,557 total genes, respectively), as identified in BadiRate analyses performed using tree 1, tree 2 and the intersection of both trees, are displayed in Supplementary Tables 15, 16 and 17, respectively. Similarly, differential representation of GO generic terms among 2,716 *Cephalotus*-specific singletons, 237 *Cephalotus*-specific two-gene families (474 total genes) and *Cephalotus*-specific 201 multigene families (1,714 total genes) are shown in Supplementary Tables 19, 20 and 21, respectively. Finally, differential representation of GO generic terms among five pairs of genes unique to *Cephalotus* and *U. gibba* is presented in Supplementary Table 18. We performed significance analyses of differential distribution of GO terms by comparing different subsets of genes with the entire complement of genes in the genome using Fisher's exact test (see for example, ref.⁴). To control for multiple testing, the resulting *P* values were corrected according to ref.⁶³.

Selection of differentially expressed genes. Strand-specific RNA-seq reads were mapped to gene models on the genome assembly using Tophat2⁶⁴ with minimum and maximum intron lengths of 20 and 20,000 bp, respectively (Supplementary Table 9). Transcript abundances calculated by featureCounts⁶⁵ were normalized using the iterative differentially expressed gene elimination strategy (iDEGES)⁶⁶, which consists of sequential TMM-(edgeR-TMM)_n normalization^{67,68}. Using the normalized reads per million mapped reads (RPM) values, differentially expressed genes were identified by an exact test for a negative binomial distribution⁶⁹ and subsequent multiple correction by adjusting the false discovery rate to *q* < 0.01 (ref.⁶³; Fig. 2c,d and Supplementary Figs 2–5 and 9). Normalized RPM values are used in Fig. 2c,d, whereas unnormalized RPM values are plotted in Supplementary Figs 2–5 and 9. The significantly differentially expressed genes were subjected to a subsequent GO-enrichment analysis (Supplementary Tables 22 and 23).

Protein sequencing of digestive fluids. Digestive fluids of *C. follicularis*, *D. adela*, *N. alata* and *S. purpurea* were collected from soil-grown plants in a greenhouse. Fluids were freeze dried and stored at room temperature. Dried samples were dissolved in a protease inhibitor cocktail (cOmplete, Mini, EDTA-free, Roche), precipitated with 8% trichloroacetic acid (TCA) and then washed with 90% acetone. They were dissolved in SDS sample buffer (62.5 mM Tris-HCl, 2% SDS, 0.25% BPB, 10% glycerol, 5% 2-mercaptoethanol, pH 6.8), denatured at 95 °C for 3 min and then separated by 12% SDS-polyacrylamide gel electrophoresis. Negative staining was performed using the Gel-Negative Stain Kit (Nacalai Tesque) according to the manufacturer's instructions. After destaining, proteins were transferred to polyvinylidene difluoride (PVDF) membranes. N-terminal sequences of each protein band were determined by the Edman degradation method using an ABI Procise 494-HT instrument (Applied Biosystems).

To obtain internal protein sequences, protein bands were dissected from the gel, destained, dehydrated with 100% acetonitrile for 5 min, dried using an evaporator and then reduced by incubating in 10 mM DTT and 25 mM ammonium bicarbonate at 56 °C for 60 min. After washing with 25 mM ammonium bicarbonate, the proteins were alkylated in 55 mM iodoacetamide and 25 mM ammonium bicarbonate for 45 min at room temperature. After washing with 50% acetonitrile containing 25 mM ammonium bicarbonate, the samples were dried using an evaporator. The proteins were in-gel-digested with 10 ng μl⁻¹ trypsin in 50 mM ammonium bicarbonate, 10 ng μl⁻¹ lysyl endopeptidase in 25 mM Tris-HCl (pH 9.0) or 20 ng μl⁻¹ V8 protease in 50 mM phosphate buffer (pH 7.8) at 37 °C overnight. The digested peptides were extracted twice by sonication in 50% acetonitrile containing 5% trifluoroacetic acid (TFA) for 10 min. The peptides were separated by high-performance liquid chromatography (HPLC) using the Pharmacia SMART System and a reverse-phase column (μRPC C2/C18 PC 3.2/3, GE Healthcare Life Sciences, or XBridge C8 5 μm 2.1 × 100 mm, Waters) under the following conditions: constant flow rate of 200 μl min⁻¹; solvent A, 0.5% TFA, solvent B, acetonitrile containing 0.5% TFA; linear gradient from 10 to 40% (B over A in % (v/v)) over 30 min (1% min⁻¹). Separated peptides were then used for protein sequencing by the Edman degradation method.

Transcriptome assembly and identification of transcripts encoding

biochemically identified proteins. RNA-seq reads of *D. adela*, *N. alata*, and *S. purpurea* (Supplementary Table 8) were assembled into transcripts using Trinity (version r2013-02-25)⁷⁰ with a 200 bp minimum contig length cut-off. Partial amino acid sequences of digestive fluid proteins were subjected to TBLASTN searches⁷¹ against the transcriptome assemblies and the *Cephalotus* gene models to identify the corresponding transcripts (Supplementary Tables 25–28). Sequence variants within a Trinity's component were considered as originating from the same gene.

Preparation of digestive fluid protein data sets. In addition to proteins identified in this study (Supplementary Tables 25–28), we obtained for phylogenetic analyses a number of previously published sequences of digestive fluid proteins^{8,9,72–78} (Supplementary Table 24). Although many protein and transcript sequences for possible digestive enzymes are available (for example, refs^{17,79–84}), we included only genes for which complete coding sequences were available and for which their presence in digestive fluid had been biochemically validated (Supplementary Table 24, last searched 20 January 2016).

Phylogenetic analyses of gene families. Phylogenetic relationships of digestive enzyme genes and other carnivory-related genes were analysed along with their homologues in the annotated genomes of ten angiosperm species (Supplementary Table 11). TBLASTX searches⁷¹ were performed against the above coding sequence (CDS) data sets with an E-value cut-off of 10. After sequence retrieval, multiple alignments were prepared using MAFFT 6.956⁸⁵, and ambiguous codons were removed using trimAl⁵⁷ implemented in Phylogears2-2.0.2013.03.15 (<http://www.fifthdimension.jp/products/phylogears/>) with the 'gappyout' option. Poorly aligned sequences were removed using MaxAlign⁸⁶. Phylogenetic trees were reconstructed by the maximum-likelihood method using RAxML v8.0.26⁵¹ with the general time-reversible (GTR) model of nucleotide substitution and four discrete gamma categories of rate heterogeneity ('GTRGAMMA' option). Support for nodes was estimated by rapid bootstrapping with 100 replicates. Trees were rooted at the midpoint between the two most divergent genes. Gene duplication events shown in Figs 2b and 3a were inferred on the basis of species overlap between partitions⁸⁷ using a Python package 'ETE3'⁸⁸. The trees were visualized using iTOL⁸⁹.

Detection of orthologous relationships. Orthology of *Cephalotus* genes and digestive enzyme genes was inferred on the basis of tree topologies reconstructed by the maximum-likelihood method using the ten plant genomes described above (Supplementary Figs 2, 4 and 5). As we cannot exclude the possibility of parallel gene losses, a clade containing genes from at least five plant genomes was designated as a putative orthologous unit.

Expression profiling of *Arabidopsis* genes. Affymetrix ATH1 (25K) microarray data sets on stress-related experiments were retrieved from ArrayExpress⁹⁰ if two or more replicates were available on wild-type *Arabidopsis* plants (Supplementary Table 30). Robust multi-array average normalized expression data⁹¹ were subjected to heatmap visualization using the R package 'gplots'. Dendrograms were constructed using the furthest neighbour method with Euclidian distances. Significance of differential expression was analysed by a randomization test with 10,000 iterations in which resamplings were performed in each gene family and the sum of expression changes was compared with the original value.

Evaluation of detection methods for molecular convergence. To evaluate different tree reconstruction methods, simulated gene sequences were generated using the R package 'Phylosim'⁹². We used publicly available simulated data sets for 16 fungi species^{93,94}. These data sets contain 1,000 simulated tree topologies of gene families, each of which was generated under observed gene duplication

and loss rates. Sequences of 300 codons were simulated on the tree topologies of the fungi data set. Codon usage was sampled from the actual frequencies in *Saccharomyces cerevisiae*⁹⁵. The κ (transition/transversion rate) was set to 1. The ω (nonsynonymous / synonymous nucleotide substitution rate ratio (dN/dS)) of each codon position was randomly sampled from a gamma distribution (shape = 0.5, rate = 1). To mimic molecular convergence, two genes were randomly selected to be converged. In terminal branches of selected genes, codon usage of *S. cerevisiae* was replaced with a biased matrix in which frequencies of codons coding for two randomly selected amino acids were increased. Increased frequency was calculated by multiplying the original value by 100, and then total frequencies of all codons were scaled to 1.

Gene trees were inferred by the maximum-likelihood method⁵¹ using first, second, third and all codon positions as well as 300 nucleotide random sequences. To obtain a robust tree topology, the gene trees were reconciled with the species tree using Treefix 1.1.10⁹⁴, which incorporates duplication-loss parsimony and a test statistic for likelihood equivalence. Reconciliation was accomplished using default settings for which 1,000 iterations of topology searches were performed and rearrangements were accepted when likelihood was not significantly reduced by the Shimodaira–Hasegawa test⁹⁶ (P value threshold of 0.05). Branch lengths of reconciled trees were optimized using RAXML⁵¹. Finally, the numbers of convergent and divergent substitutions were estimated from the inferred tree topologies and the original simulated alignments using CodeMLancestral²¹ (Supplementary Fig. 10). Substitution pairs that result in the same descendant amino acid at the same alignment position in both branches were categorized as convergent changes, whereas the remaining substitution pairs were counted as divergent changes^{21,28}.

Detection of molecular convergence in digestive fluid proteins. Genes encoding digestive fluid proteins identified in this study (Supplementary Tables 25–28) and previous research (Supplementary Table 24) were analysed. When corresponding gene sequences for a given species clustered together in the maximum-likelihood trees (Supplementary Fig. 5), they were considered to represent the same gene, whereafter we retained our own sequences to circumvent incorrect inference of gene duplication events in phylogeny reconciliation. A maximum-likelihood tree was reconstructed using third codon position sequences of the trimAl-processed alignments, and it was subsequently reconciled with a species tree prepared from a dated large-scale plastid phylogeny of flowering plants⁵⁴ using Treefix⁹⁴ with default parameters, except with the number of iterations increased to 1,000. Although the plastid-based topology⁵⁴ is partly different from nuclear-based topology^{52,53} (Supplementary Fig. 1h), we employed it because of the necessity to include carnivorous lineages in which nuclear genome sequences are unavailable (for example, *Drosera*, *Nepenthes* and *Sarracenia*). Branch lengths of the reconciled trees were optimized against trimAl-processed CDS alignments using RAXML⁵¹. The trees were subsequently used for Bayesian ancestral state reconstruction using PhyloBayes⁹⁷ over 12,000 generations (2,000 generations of burn-in) with an infinite mixture of GTR substitution models (CAT-GTR model) of amino acid substitution and five discrete gamma categories of rate heterogeneity to calculate posterior numbers of convergent and divergent substitution pairs. Background levels (null hypothesis) of convergent substitution pairs were estimated by a linear regression in which the posterior numbers of convergent changes were predicted by divergent changes²¹. Over-accumulation of convergent changes in a tree was examined by one-sided single-sample proportion tests⁹⁸ with Yate's continuity correction⁹⁹ and subsequent Bonferroni adjustment for multiple comparisons¹⁰⁰. Digestive enzyme branch pairs among independent carnivorous plant lineages were examined in the statistical test. Corrected P values are shown in Fig. 3b and Supplementary Fig. 6.

Homology modelling of protein structures. Protein structures of digestive enzymes were analysed using the SWISS-MODEL Workspace¹⁰¹. Template models were selected using the 'Template Identification' tool. SWISS-MODEL Template Library IDs of selected templates were 2dkv.1.A, 3zk4.1.A and 1dix.1.A for GH19 chitinases, purple acid phosphatases and RNase T2s, respectively. Predicted models were visualized using UCSF Chimera 1.10¹⁰². Relative exposure of amino acid surfaces was calculated by dividing solvent-accessible surface in protein structures by the theoretical maximum of corresponding amino acids in Gly-X-Gly tripeptide contexts¹⁰³. The relative solvent-accessible surface area for a paired amino acid substitution was reported by averaging values in proteins constituting the two clades (Supplementary Fig. 8).

Data availability. The *Cephalotus* genome assembly and gene models are available from the DNA Data Bank of Japan (DDBJ) with the accession numbers BDDD01000001 to BDDD01016307. The genomic sequences, gene models and other source data are also available at CoGe (Genome ID = 29002) and Dryad (doi:10.5061/dryad.50tq3). The DDBJ accession numbers for DNA-seq (DRR053706–DRR053720), mRNA-seq (DRR053690–DRR051749; DRR029007–DRR29010) and small RNA-seq (DRR058704–DRR058708) are shown in Supplementary Tables 1, 8 and 10, respectively. DDBJ accessions and gene IDs for coding sequences of digestive fluid proteins are provided in Supplementary Tables 25–28.

Received 12 July 2016; accepted 16 December 2016;
published 6 February 2017

References

- Juniper, B. E., Robins, R. J. & Joel, D. M. *The Carnivorous Plants* (Academic, 1989).
- Darwin, C. *Insectivorous Plants* (D. Appleton and Company, 1875).
- Albert, V. A., Williams, S. E. & Chase, M. W. Carnivorous plants: phylogeny and structural evolution. *Science* **257**, 1491–1495 (1992).
- Denoeud, F. *et al.* The coffee genome provides insight into the convergent evolution of caffeine biosynthesis. *Science* **345**, 1181–1184 (2014).
- Jaillon, O. *et al.* The grapevine genome sequence suggests ancestral hexaploidization in major angiosperm phyla. *Nature* **449**, 463–467 (2007).
- Li, L., Stoeckert, C. J. & Roos, D. S. OrthoMCL: identification of ortholog groups for eukaryotic genomes. *Genome Res.* **13**, 2178–2189 (2003).
- Gallie, D. R. & Chang, S. C. Signal transduction in the carnivorous plant *Sarracenia purpurea*. Regulation of secretory hydrolase expression during development and in response to resources. *Plant Physiol.* **115**, 1461–1471 (1997).
- Okabe, T., Yoshimoto, I., Hitoshi, M., Ogawa, T. & Ohyama, T. An S-like ribonuclease gene is used to generate a trap-leaf enzyme in the carnivorous plant *Drosera adelae*. *FEBS Lett.* **579**, 5729–5733 (2005).
- Nishimura, E. *et al.* S-like ribonuclease gene expression in carnivorous plants. *Planta* **238**, 955–967 (2013).
- Ellison, A. M. Nutrient limitation and stoichiometry of carnivorous plants. *Plant Biol.* **8**, 740–747 (2006).
- Król, E. *et al.* Quite a few reasons for calling carnivores 'the most wonderful plants in the world'. *Ann. Bot.* **109**, 47–64 (2012).
- Adlassnig, W., Peroutka, M. & Lendl, T. Traps of carnivorous pitcher plants as a habitat: composition of the fluid, biodiversity and mutualistic activities. *Ann. Bot.* **107**, 181–194 (2011).
- Whitney, H. M. & Federle, W. Biomechanics of plant–insect interactions. *Curr. Opin. Plant Biol.* **16**, 105–111 (2013).
- Bak, S. *et al.* Cytochromes P450. *Arab. B.* **9**, e0144 (2011).
- Li, F. *et al.* Identification of the wax ester synthase/acyl-coenzyme A: diacylglycerol acyltransferase WSD1 required for stem wax ester biosynthesis in *Arabidopsis*. *Plant Physiol.* **148**, 97–107 (2008).
- Buch, F. *et al.* Secreted pitfall-trap fluid of carnivorous *Nepenthes* plants is unsuitable for microbial growth. *Ann. Bot.* **111**, 375–383 (2013).
- Schulze, W. X. *et al.* The protein composition of the digestive fluid from the Venus flytrap sheds light on prey digestion mechanisms. *Mol. Cell. Proteomics* **11**, 1306–1319 (2012).
- Michalko, J. *et al.* Glucan-rich diet is digested and taken up by the carnivorous sundew (*Drosera rotundifolia* L.): implication for a novel role of plant β -1,3-glucanases. *Planta* **238**, 715–725 (2013).
- Bemm, F. *et al.* Venus flytrap carnivorous lifestyle builds on herbivore defense strategies. *Genome Res.* **26**, 1–14 (2016).
- Heubl, G., Bringmann, G. & Meimberg, H. Molecular phylogeny and character evolution of carnivorous plant families in Caryophyllales — revisited. *Plant Biol.* **8**, 821–830 (2006).
- Castoe, T. A. *et al.* Evidence for an ancient adaptive episode of convergent molecular evolution. *Proc. Natl Acad. Sci. USA* **106**, 8986–8991 (2009).
- Michalak, P. Coexpression, coregulation, and cofunctionality of neighboring genes in eukaryotic genomes. *Genomics* **91**, 243–248 (2008).
- Stewart, C. B., Schilling, J. W. & Wilson, A. C. Adaptive evolution in the stomach lysozymes of foregut fermenters. *Nature* **330**, 401–404 (1987).
- Zhang, J. Parallel adaptive origins of digestive RNases in Asian and African leaf monkeys. *Nat. Genet.* **38**, 819–823 (2006).
- Choi, S. S., Vallender, E. J. & Lahn, B. T. Systematically assessing the influence of 3-dimensional structural context on the molecular evolution of mammalian proteomes. *Mol. Biol. Evol.* **23**, 2131–2133 (2006).
- Bustamante, C. D., Townsend, J. P. & Hartl, D. L. Solvent accessibility and purifying selection within proteins of *Escherichia coli* and *Salmonella enterica*. *Mol. Biol. Evol.* **17**, 301–308 (2000).
- Goldman, N., Thorne, J. L. & Jones, D. T. Assessing the impact of secondary structure and solvent accessibility on protein evolution. *Genetics* **149**, 445–458 (1998).
- Goldstein, R. A., Pollard, S. T., Shah, S. D. & Pollock, D. D. Nonadaptive amino acid convergence rates decrease over time. *Mol. Biol. Evol.* **32**, 1373–1381 (2015).
- Ellison, A. M. & Gotelli, N. J. Energetics and the evolution of carnivorous plants—Darwin's 'most wonderful plants in the world'. *J. Exp. Bot.* **60**, 19–42 (2009).
- Scherzer, S. *et al.* The *Dionaea muscipula* ammonium channel DmAMT1 provides NH₄⁺ uptake associated with Venus flytrap's prey digestion. *Curr. Biol.* **23**, 1649–1657 (2013).
- Murashige, T. & Skoog, F. A revised medium for rapid growth and bio assays with tobacco tissue cultures. *Physiol. Plant.* **15**, 473–497 (1962).

32. Marçais, G. & Kingsford, C. A fast, lock-free approach for efficient parallel counting of occurrences of k-mers. *Bioinformatics* **27**, 764–770 (2011).
33. Gnerre, S. *et al.* High-quality draft assemblies of mammalian genomes from massively parallel sequence data. *Proc. Natl Acad. Sci. USA* **108**, 1513–1518 (2011).
34. Boetzer, M., Henkel, C. V., Jansen, H. J., Butler, D. & Pirovano, W. Scaffolding pre-assembled contigs using SSPACE. *Bioinformatics* **27**, 578–579 (2011).
35. Luo, R. *et al.* SOAPdenovo2: an empirically improved memory-efficient short-read *de novo* assembler. *GigaScience* **1**, 18 (2012).
36. English, A. C. *et al.* Mind the gap: upgrading genomes with Pacific Biosciences RS long-read sequencing technology. *PLoS ONE* **7**, e47768 (2012).
37. Benson, G. Tandem repeats finder: a program to analyze DNA sequences. *Nucleic Acids Res.* **27**, 573–580 (1999).
38. Levin, J. Z. *et al.* Comprehensive comparative analysis of strand-specific RNA sequencing methods. *Nat. Methods* **7**, 709–715 (2010).
39. Birney, E. & Durbin, R. Using GeneWise in the *Drosophila* annotation experiment. *Genome Res.* **10**, 547–548 (2000).
40. Trapnell, C. *et al.* Transcript assembly and quantification by RNA-seq reveals unannotated transcripts and isoform switching during cell differentiation. *Nat. Biotechnol.* **28**, 511–515 (2010).
41. Mitchell, A. *et al.* The InterPro protein families database: the classification resource after 15 years. *Nucleic Acids Res.* **43**, D213–D221 (2014).
42. Quevillon, E. *et al.* InterProScan: protein domains identifier. *Nucleic Acids Res.* **33**, W116–W120 (2005).
43. Parra, G., Bradnam, K. & Korf, I. CEGMA: a pipeline to accurately annotate core genes in eukaryotic genomes. *Bioinformatics* **23**, 1061–1067 (2007).
44. Rice, P., Longden, I. & Bleasby, A. EMBOSS: the European molecular biology open software suite. *Trends Genet.* **16**, 276–277 (2000).
45. Axtell, M. J. ShortStack: comprehensive annotation and quantification of small RNA genes. *RNA* **19**, 740–751 (2013).
46. Kozomara, A. & Griffiths-Jones, S. miRBase: annotating high confidence microRNAs using deep sequencing data. *Nucleic Acids Res.* **42**, D68–D73 (2014).
47. Dsouza, M., Larsen, N. & Overbeek, R. Searching for patterns in genomic data. *Trends Genet.* **13**, 497–498 (1997).
48. Lorenz, R. *et al.* ViennaRNA package 2.0. *Algorithms Mol. Biol.* **6**, 26 (2011).
49. Jones-Rhoades, M. W. & Bartel, D. P. Computational identification of plant microRNAs and their targets, including a stress-induced miRNA. *Mol. Cell* **14**, 787–799 (2004).
50. Dai, X. & Zhao, P. X. psRNATarget: a plant small RNA target analysis server. *Nucleic Acids Res.* **39**, W155–W159 (2011).
51. Stamatakis, A. RAxML version 8: a tool for phylogenetic analysis and post-analysis of large phylogenies. *Bioinformatics* **30**, 1312–1313 (2014).
52. Zeng, L. *et al.* Resolution of deep angiosperm phylogeny using conserved nuclear genes and estimates of early divergence times. *Nat. Commun.* **5**, 4956 (2014).
53. Wickett, N. J. *et al.* Phylotranscriptomic analysis of the origin and early diversification of land plants. *Proc. Natl Acad. Sci. USA* **111**, E4859–E4868 (2014).
54. Bell, C. D., Soltis, D. E. & Soltis, P. S. The age and diversification of the angiosperms re-revisited. *Am. J. Bot.* **97**, 1296–1303 (2010).
55. Ouyang, S. & Buell, C. R. The TIGR Plant Repeat Databases: a collective resource for the identification of repetitive sequences in plants. *Nucleic Acids Res.* **32**, D360–D363 (2004).
56. Wallace, I. M., O'Sullivan, O., Higgins, D. G. & Notredame, C. M-Coffee: combining multiple sequence alignment methods with T-Coffee. *Nucleic Acids Res.* **34**, 1692–1699 (2006).
57. Capella-Gutierrez, S., Silla-Martinez, J. M. & Gabaldon, T. trimAl: a tool for automated alignment trimming in large-scale phylogenetic analyses. *Bioinformatics* **25**, 1972–1973 (2009).
58. Darriba, D., Taboada, G. L., Doallo, R. & Posada, D. ProtTest 3: fast selection of best-fit models of protein evolution. *Bioinformatics* **27**, 1164–1165 (2011).
59. Sanderson, M. J. r8s: inferring absolute rates of molecular evolution and divergence times in the absence of a molecular clock. *Bioinformatics* **19**, 301–302 (2003).
60. Librado, P., Vieira, F. G. & Rozas, J. BadiRate: estimating family turnover rates by likelihood-based methods. *Bioinformatics* **28**, 279–281 (2012).
61. Carretero-Paulet, L. *et al.* High gene family turnover rates and gene space adaptation in the compact genome of the carnivorous plant *Utricularia gibba*. *Mol. Biol. Evol.* **32**, 1284–1295 (2015).
62. Jurka, J. *et al.* Repbase Update, a database of eukaryotic repetitive elements. *Cytogenet. Genome Res.* **110**, 462–467 (2005).
63. Benjamini, Y. & Hochberg, Y. Controlling the false discovery rate: a practical and powerful approach to multiple testing. *J. R. Stat. Soc. B* **57**, 289–300 (1995).
64. Kim, D. *et al.* TopHat2: accurate alignment of transcriptomes in the presence of insertions, deletions and gene fusions. *Genome Biol.* **14**, R36 (2013).
65. Liao, Y., Smyth, G. K. & Shi, W. featureCounts: an efficient general purpose program for assigning sequence reads to genomic features. *Bioinformatics* **30**, 923–930 (2014).
66. Sun, J., Nishiyama, T., Shimizu, K. & Kadota, K. TCC: an R package for comparing tag count data with robust normalization strategies. *BMC Bioinformatics* **14**, 219 (2013).
67. Robinson, M. D. & Oshlack, A. A scaling normalization method for differential expression analysis of RNA-seq data. *Genome Biol.* **11**, 2010–2011 (2010).
68. Robinson, M. D., McCarthy, D. J. & Smyth, G. K. edgeR: a bioconductor package for differential expression analysis of digital gene expression data. *Bioinformatics* **26**, 139–140 (2010).
69. Robinson, M. D. & Smyth, G. K. Small-sample estimation of negative binomial dispersion, with applications to SAGE data. *Biostatistics* **9**, 321–332 (2008).
70. Grabherr, M. G. *et al.* Full-length transcriptome assembly from RNA-seq data without a reference genome. *Nat. Biotechnol.* **29**, 644–652 (2011).
71. Altschul, S. F., Gish, W., Miller, W., Myers, E. W. & Lipman, D. J. Basic local alignment search tool. *J. Mol. Biol.* **215**, 403–410 (1990).
72. Paszota, P. *et al.* Secreted major Venus flytrap chitinase enables digestion of Arthropod prey. *Biochim. Biophys. Acta* **2**, 374–383 (2014).
73. Takahashi, K. *et al.* A cysteine endopeptidase ('dionain') is involved in the digestive fluid of *Dionea muscipula* (Venus's fly-trap). *Biosci. Biotechnol. Biochem.* **75**, 346–348 (2011).
74. Athauda, S. B. *et al.* Enzymic and structural characterization of nepenthesin, a unique member of a novel subfamily of aspartic proteinases. *Biochem. J.* **381**, 295–306 (2004).
75. Buch, F., Pauchet, Y., Rott, M. & Mithofer, A. Characterization and heterologous expression of a PR-1 protein from traps of the carnivorous plant *Nepenthes mirabilis*. *Phytochemistry* **100**, 43–50 (2014).
76. Rottloff, S. *et al.* Functional characterization of a class III acid endochitinase from the traps of the carnivorous pitcher plant genus, *Nepenthes*. *J. Exp. Bot.* **62**, 4639–4647 (2011).
77. Hatano, N. & Hamada, T. Proteome analysis of pitcher fluid of the carnivorous plant *Nepenthes alata*. *J. Proteome Res.* **7**, 809–816 (2008).
78. Hatano, N. & Hamada, T. Proteomic analysis of secreted protein induced by a component of prey in pitcher fluid of the carnivorous plant *Nepenthes alata*. *J. Proteomics* **75**, 4844–4852 (2012).
79. Renner, T. & Specht, C. D. Molecular and functional evolution of class I chitinases for plant carnivory in the Caryophyllales. *Mol. Biol. Evol.* **29**, 2971–2985 (2012).
80. Eilenberg, H., Pnini-Cohen, S., Schuster, S., Movtchan, A. & Zilberstein, A. Isolation and characterization of chitinase genes from pitchers of the carnivorous plant *Nepenthes khasiana*. *J. Exp. Bot.* **57**, 2775–2784 (2006).
81. Matusíková, I. *et al.* Tentacles of *in vitro*-grown round-leaf sundew (*Drosera rotundifolia* L.) show induction of chitinase activity upon mimicking the presence of prey. *Planta* **222**, 1020–1027 (2005).
82. An, C.-I., Fukusaki, E. & Kobayashi, A. Aspartic proteinases are expressed in pitchers of the carnivorous plant *Nepenthes alata* Blanco. *Planta* **214**, 661–667 (2002).
83. Srivastava, A., Rogers, W. L., Breton, C. M., Cai, L. & Malmberg, R. L. Transcriptome analysis of *Sarracenia*, an insectivorous plant. *DNA Res.* **18**, 253–261 (2011).
84. Jensen, M. K. *et al.* Transcriptome and genome size analysis of the Venus flytrap. *PLoS ONE* **10**, e0123887 (2015).
85. Katoh, K. & Standley, D. M. MAFFT multiple sequence alignment software version 7: improvements in performance and usability. *Mol. Biol. Evol.* **30**, 772–780 (2013).
86. Gouveia-Oliveira, R., Sackett, P. W. & Pedersen, A. G. MaxAlign: maximizing usable data in an alignment. *BMC Bioinformatics* **8**, 312 (2007).
87. Huerta-Cepas, J. *et al.* The human phylome. *Genome Biol.* **8**, 934–941 (2007).
88. Huerta-Cepas, J., Serra, F. & Bork, P. ETE 3: reconstruction, analysis, and visualization of phylogenomic data. *Mol. Biol. Evol.* **33**, 1635–1638 (2016).
89. Letunic, I. & Bork, P. Interactive Tree Of Life v2: online annotation and display of phylogenetic trees made easy. *Nucleic Acids Res.* **39**, W475–W478 (2011).
90. Kolesnikov, N. *et al.* ArrayExpress update—simplifying data submissions. *Nucleic Acids Res.* **43**, D1113–D1116 (2015).
91. Irizarry, R. A. *et al.* Exploration, normalization, and summaries of high density oligonucleotide array probe level data. *Biostatistics* **4**, 249–264 (2003).
92. Sipos, B., Massingham, T., Jordan, G. E. & Goldman, N. PhyloSim - Monte Carlo simulation of sequence evolution in the R statistical computing environment. *BMC Bioinformatics* **12**, 104 (2011).
93. Rasmussen, M. D. & Kellis, M. A Bayesian approach for fast and accurate gene tree reconstruction. *Mol. Biol. Evol.* **28**, 273–290 (2011).
94. Wu, Y. C., Rasmussen, M. D., Bansal, M. S. & Kellis, M. TreeFix: statistically informed gene tree error correction using species trees. *Syst. Biol.* **62**, 110–120 (2013).
95. Nakamura, Y., Gojobori, T. & Ikemura, T. Codon usage tabulated from international DNA sequence databases: status for the year 2000. *Nucleic Acids Res.* **28**, 292 (2000).

96. Shimodaira, H. & Hasegawa, M. Multiple comparisons of log-likelihoods with applications to phylogenetic inference. *Mol. Biol. Evol.* **16**, 1114–1116 (1999).
97. Lartillot, N., Lepage, T. & Blanquart, S. PhyloBayes 3: a Bayesian software package for phylogenetic reconstruction and molecular dating. *Bioinformatics* **25**, 2286–2288 (2009).
98. Wilson, E. B. Probable inference, the law of succession, and statistical inference. *J. Am. Stat. Assoc.* **22**, 209–212 (1927).
99. Yates, F. Contingency tables involving small numbers and the χ^2 test. *J. R. Stat. Soc.* **1**(suppl.) 217–235 (1934).
100. Neyman, J. & Pearson, E. S. On the use and interpretation of certain test criteria for purposes of statistical inference: part I. *Biometrika* **20A**, 175–240 (1928).
101. Biasini, M. *et al.* SWISS-MODEL: modelling protein tertiary and quaternary structure using evolutionary information. *Nucleic Acids Res.* **42**, W252–W258 (2014).
102. Pettersen, E. F. *et al.* UCSF Chimera — a visualization system for exploratory research and analysis. *J. Comput. Chem.* **25**, 1605–1612 (2004).
103. Tien, M. Z., Meyer, A. G., Sydykova, D. K., Spielman, S. J. & Wilke, C. O. Maximum allowed solvent accessibilities of residues in proteins. *PLoS ONE* **8**, e80635 (2013).

Acknowledgements

We acknowledge the following sources for funding: MEXT/JSPS KAKENHI grant numbers 12J04926 (K.F.), 22128008 (T.N.), 221S0002 (M.K.), 16370102 (M.H.), 22128001 (M.H.) and 22128002 (M.H.); MECS CGL2013-45211 (J.R.), R01 GM097251 (D.D.P.), and the US NSF 0922742 and 1442190 (V.A.A.). The sequence data are archived at DDBJ and CoGe. This work was supported by MPRF-NIBB, I. Kajikawa and Y. Matsuzaki for cultivation, J. G. Conran and M. Waycott for locality observation and FGF-NIBB, Y. Makino, S. Ooi and K. Yamaguchi for experiments. Computations were partially performed on the NIG supercomputer and DIAF-NIBB.

Author contributions

K.F., N.S. and M.H. maintained and collected samples. K.F. and M.H. established culture conditions to control the leaf dimorphism. K.F., X.F., T.N., S.L., and M.H. coordinated genome assembly and annotation. K.F., X.F., C.C., M.N., S.S. and M.X. prepared and sequenced Illumina libraries. M.N. coordinated

PacBio sequencing. T.F.S. performed PacBio sequencing. T.I. and M.K. performed error correction of PacBio reads and inter-contig gap filling. K.F., X.F., H.C. and L.M. performed gene prediction and annotation. K.F. performed miRNA prediction and annotation. D.A.-P. performed singleton gene analysis. C.Z. and D.S. performed synteny analysis. P.L., A.S.-G and J.R. performed BadiRate analysis. L.C.-P. and V.A.A. performed GO-enrichment analysis. K.F., K.M.F., T.-H.C. and G.P. performed gene family analysis. T.F., Y. Hiwatashi, Y. Hoshi, H.M., N.S., T.U. and M.H. performed digestive fluid sampling and protein sequencing. K.F., S.T.P. and D.D.P. performed convergence analysis. K.F., V.A.A. and M.H. wrote the paper with input from all authors. M.H. initiated and directed the project. K.F., V.A.A., S.L. and M.H. are representatives of each group. K.F. and X.F. should be considered joint first authors.

Additional information

Supplementary information is [available for this paper](#).

Reprints and permissions information is available at www.nature.com/reprints.

Correspondence and requests for materials should be addressed to K.F., V.A.A., S.L. or M.H.

How to cite this article: Fukushima, K. *et al.* Genome of the pitcher plant *Cephalotus* reveals genetic changes associated with carnivory. *Nat. Ecol. Evol.* **1**, 0059 (2017).

Competing interests

The authors declare no competing financial interests.



This article is licensed under a Creative Commons Attribution 4.0 International License, which permits use, sharing, adaptation, distribution and reproduction in any medium or format, as long as you give appropriate credit to the original author(s) and the source, provide a link to the Creative Commons license, and indicate if changes were made.

The images or other third party material in this article are included in the article's Creative Commons license, unless indicated otherwise in a credit line to the material. If material is not included in the article's Creative Commons license and your intended use is not permitted by statutory regulation or exceeds the permitted use, you will need to obtain permission directly from the copyright holder. To view a copy of this license, visit <http://creativecommons.org/licenses/by/4.0/>